Biochimica et Biophysica Acta 1862 (2016) 1710–1723

Contents lists available at ScienceDirect

Biochimica et Biophysica Acta

journal homepage: www.elsevier.com/locate/bbadis

Cyclooxygenase-2 expression in hepatocytes attenuates non-alcoholic steatohepatitis and liver fibrosis in mice

Omar Motiño [a,1], Noelia Agra [a,1], Rocío Brea Contreras [a,1], Marina Domínguez-Moreno [a], Carmelo García-Monzón [b], Javier Vargas-Castrillón [b], Cristina E. Carnovale [c], Lisardo Boscá [a,f], Marta Casado [d,f], Rafael Mayoral [f,g], M. Pilar Valdecantos [a], Ángela M. Valverde [a,e], Daniel E. Francés [c,*,2], Paloma Martín-Sanz [a,f,**,2]

[a] Instituto de Investigaciones Biomédicas (IIB) "Alberto Sols", CSIC-UAM, Arturo Duperier 4, 28029 Madrid, Spain
[b] Liver Research Unit, Hospital Universitario Santa Cristina, Instituto de Investigación Sanitaria Princesa, Amadeo Vives 2, 28009 Madrid, Spain
[c] Instituto de Fisiología Experimental (IFISE-CONICET), Suipacha 570, 2000 Rosario, Argentina
[d] Instituto de Biomedicina de Valencia, IBV-CSIC, Jaume Roig 11, 46010 Valencia, Spain
[e] Centro de Investigación Biomédica en Red de Diabetes y Enfermedades Metabólicas Asociadas (CIBERdem), Monforte de Lemos 3-5, 28029 Madrid, Spain
[f] Centro de Investigación Biomédica en Red de Enfermedades Hepáticas y Digestivas (CIBERehd), Monforte de Lemos 3-5, 28029 Madrid, Spain
[g] Department of Medicine, University of California, San Diego, 9500 Gilman Drive, La Jolla, CA 92093, USA

ARTICLE INFO

Article history:
Received 1 March 2016
Received in revised form 7 June 2016
Accepted 13 June 2016
Available online 15 June 2016

Keywords:
COX-2
Liver
Steatohepatitis
Inflammation
Fibrosis

ABSTRACT

Cyclooxygenase-2 (COX-2) is involved in different liver diseases but little is known about the significance of COX-2 in the development and progression of non-alcoholic steatohepatitis (NASH). This study was designed to elucidate the role of COX-2 expression in hepatocytes in the pathogenesis of steatohepatitis and hepatic fibrosis. In the present work, hepatocyte-specific COX-2 transgenic mice (hCOX-2-Tg) and their wild-type (Wt) littermates were either fed methionine-and-choline deficient (MCD) diet to establish an experimental non-alcoholic steatohepatitis (NASH) model or injected with carbon tetrachloride (CCl_4) to induce liver fibrosis. In our animal model, hCOX-2-Tg mice fed MCD diet showed lower grades of steatosis, ballooning and inflammation than Wt mice, in part by reduced recruitment and infiltration of hepatic macrophages, with a corresponding decrease in serum levels of pro-inflammatory cytokines. Furthermore, hCOX-2-Tg mice showed a significant attenuation of the MCD diet-induced increase in oxidative stress and hepatic apoptosis observed in Wt mice. Even more, hCOX-2-Tg mice treated with CCl_4 had significantly lower stages of fibrosis and less hepatic content of collagen, hydroxyproline and pro-fibrogenic markers than Wt controls. Collectively, our data indicates that constitutive hepatocyte COX-2 expression ameliorates NASH and liver fibrosis development in mice by reducing inflammation, oxidative stress and apoptosis and by modulating activation of hepatic stellate cells, respectively, suggesting a possible protective role for COX-2 induction in NASH/NAFLD progression.

1. Introduction

Cyclooxygenase-1 (COX-1) and -2 catalyze the first step in prostanoid biosynthesis. COX-1 is constitutively expressed in many tissues, whereas COX-2 is induced by a variety of stimuli [1]. Adult hepatocytes fail to induce COX-2 expression regardless of the pro-inflammatory factors used [2]. However, our group and others demonstrated that partial hepatectomy (PH) induced COX-2 in hepatocytes and contributed to

Abbreviations: COX-2, cyclooxygenase-2; PGE_2, prostaglandin E_2;; RCD, regular chow diet; MCD, methionine and choline deficient diet; CCl_4, carbon tetrachloride; NAFLD, non-alcoholic fatty liver disease; NL, normal liver; NAS, non-alcoholic steatosis; NASH, non-alcoholic steatohepatitis; TG, triglycerides; ALT, alanine transaminase; IL-6, interleukin 6; IL-1β, interleukin 1β; TNF-α, tumor necrosis factor α; TGF-β1, transforming growth factor β1; MCP-1, monocyte chemotactic protein-1; CCR2, C-C chemokine receptor type 2; Ly6C, lymphocyte antigen 6C; Bax, Bcl-2-associated X protein; Bcl-x_L, B-cell lymphoma-extra-large; Mcl-1, myeloid cell leukemia 1;; DFU, (5,5-dimethyl-3(3-fluorophenyl)-4-(4-methylsulfonyl)phenyl-2(5H)-furanone); *Cat*, catalase; *Sod1*, superoxide dismutase 1; *Sod 2*, superoxide dismutase 2; *Gsr*, glutathione reductase; α-SMA, alpha smooth muscle actin; Col1a1, Collagen type I alpha 1; PDGFRA, platelet-derived growth factor receptor alpha; PDGFRB, platelet-derived growth factor receptor beta; PDGFA, platelet-derived growth factor alpha; PDGFB, platelet-derived growth factor beta; HGF, hepatocyte growth factor.

* Corresponding author.
** Correspondence to: P. Martín-Sanz, Instituto de Investigaciones Biomédicas (IIB) "Alberto Sols", CSIC-UAM, Arturo Duperier, 4, 28029 Madrid, Spain.
E-mail addresses: frances@ifise-conicet.gov.ar (D.E. Francés), pmartins@iib.uam.es (P. Martín-Sanz).
[1] These authors contributed equally to this work.
[2] These two authors share senior authorship.

http://dx.doi.org/10.1016/j.bbadis.2016.06.009
0925-4439/

the progression of cell cycle during regeneration [3]. In addition, expression of COX-2 has been detected in several liver pathologies [4]. On the other hand, hepatocyte-specific expression of COX-2 exerts an efficient protection against acute liver injury by an antiapoptotic/antinecrotic effect and by accelerated early hepatocyte proliferation [5].

Non-alcoholic fatty liver disease (NAFLD) encompasses from non-alcoholic steatosis (NAS), a simple accumulation of fat in hepatocytes, to non-alcoholic steatohepatitis (NASH), which is characterized by lobular and portal inflammation, hepatocyte ballooning and variable degrees of fibrosis [6]. NAFLD worldwide prevalence in general population is estimated to be 20–30% in Western Countries and 5–18% in Asia and is increasing over time [7]. The causes of progression from NAS to NASH remain unclear, but lipotoxicity, oxidative stress, apoptosis and an imbalance of pro- and anti-inflammatory cytokines are believed to play key roles [8,9]. Activated Kupffer and hepatic stellate cells (HSC) contribute to pro-inflammatory cytokines production during NASH, particularly tumor necrosis factor (TNF-α) and interleukin 6 (IL-6) [10]. NASH, in turn, can progress to fibrosis and the main cell type responsible for extracellular matrix (ECM) deposition are activated HSCs; moreover, hepatocytes are replaced by scar tissue composed primarily of type I collagen produced by HSCs [11]. Induction of alpha-smooth muscle actin (α-SMA) is the single most reliable marker of HSC activation that secrete TGF-β1 and respond to this cytokine increasing type I collagen deposition [12]. Hepatic TGF-β1 expression is increased in animal models of liver fibrosis and in patients with chronic liver diseases [13] and has been inversely correlated to prostaglandin E_2 (PGE_2) action over HSCs activation [14].

Regarding COX-2 and the impact of PGE_2 on the development of NASH the data are controversial. Some studies indicate that PGs favor the development of hepatic steatosis, NASH and ultimately fibrosis [15–17], whilst others provide evidence that PGE_2 suppresses fibrogenesis and NASH progression since COX-2 inhibition potentiates inflammation and experimental liver fibrosis [14,18,19]. Our previous results indicate that constitutive expression of COX-2 in hepatocytes protects against high fat diet-induced steatosis, inflammation, obesity and insulin resistance [20]. These findings prompted us to screen the role of hepatic-specific COX-2 expression in a murine model of NASH and fibrosis induced by MCD and CCl_4, respectively.

In the present study we have demonstrated that expression of COX-2 in hepatocytes protects against NASH development by attenuating steatosis and inflammation and by inhibiting apoptotic pathways. Moreover, hepatocyte COX-2 expression was able to diminish the induction of profibrogenic markers and reduce the progression of the CCl_4-induced fibrotic process by restricting HSC activation and ECM deposition. These data confirm that constitutive COX-2 expression has a hepatoprotective role in NASH and liver fibrosis murine models.

2. Material and methods

2.1. Chemicals

Antibodies were from Santa Cruz Biotechnology (Dallas, TX, USA), Sigma Aldrich (St. Louis, MO, USA), Cell Signaling (Danvers, MA, USA) and Cayman Chemical (Ann Arbor, MI, USA). Reagents were from Roche Diagnostics (Basel, Switzerland) or Sigma Chemical Co. Reagents for electrophoresis were obtained from Bio-Rad (Hercules, CA, USA). Tissue culture dishes were from Falcon (Becton Dickinson Labware, Franklin Lakes, NJ, USA). Tissue culture media were from Gibco (Life Technologies™, Carlsbad, CA, USA).

2.2. Animal experimentation

hCOX-2-Tg mice and their corresponding wild type (Wt) littermates were generated by systematic mating of the heterozygous B6D2-Tg (APOE-PTGS2/4)Upme expressing 55 copies of transgene with B6D2F1/OlaHsd Wt mice in our animal house for more than seven generations. The hCOX-2-Tg animals were phenotypically similar to their normal litter-mates and did not exhibit a detectable histological change in the liver at 12-weeks of age. Integration of transgene was systematically checked by PCR analysis of genomic tail DNA. Transgenic mice (hCOX-2-Tg) constitutively express human COX-2 in hepatocytes under the control of the human ApoE promoter and its specific hepatic control region (HCR), a unique regulatory domain that directs ApoE expression in the liver [21], lacking macrophage-specific regulatory regions (ME.2 and ME.1) [22]. The animals were maintained in light/dark (12 h light/12 h dark), temperature (22 °C) and humidity-controlled rooms with free access to drinking water. Mice were fed with regular chow diet (RCD; SAFE A04-10 Panlab, Barcelona) or methionine choline-deficient diet (MCD; TD-90262 Harland-Tecklad, Indianapolis, IN) for 2 and 4 weeks. Some of the Wt and hCOX-2-Tg mice ($n = 6$) were fed with MCD diet for 4 weeks and then with RCD diet for another 5 days as a diet recovery model (reverse protocol) (R). To induce fibrosis, CCl_4 (1:4 in olive oil) was intraperitoneally (i.p.) administered to hCOX-2-Tg and Wt mice at a dose of 1.6 ml/kg body weight twice-weekly. Control animals were i.p. injected with olive oil. During MCD diet treatment, body weight and food intake were examined every two days. 2 wk, 4 wk and 4 wk + R after MCD diet or 9 wk after CCl_4 treatment, the animals were sacrificed and the liver was snap-frozen in liquid nitrogen and stored at −80 °C, collected in a solution containing 30% sucrose in PBS or fixed in 10% buffered formalin. Plasma was obtained from the inferior cava vein.

All animal experimentation was controlled following the recommendations of the Federation of European Laboratory Animal Science Associations (FELASA) on health monitoring, and of the National Institutes of health guide for the care and use of laboratory animals (NIH Publications No. 8023, revised 1978) whereas use of animals in experimental procedures was approved by the Institutional Care Instructions (Bioethical Commission from Spanish National Research Council, Spain).

2.3. Histopathology assessment

Hematoxylin-Eosin (H&E) and Masson's trichrome-stained (MTC) paraffin-embedded liver biopsy sections from studied mice were evaluated by the same experienced liver pathologist (J.V-C) blinded to the features of animal groups. The NAFLD activity score (NAS) and the fibrosis stage was assessed using the NAFLD scoring system for mice models validated by Liang et al. [23]. Briefly, steatosis was graded as follows: grade 0, <5% of steatotic hepatocytes; grade 1, 5–33%; grade 2, >33–66%; and grade 3, >66%. Lobular inflammation was scored as follows: 0, no foci; 1, 0.5–1 foci; 2, 1–2 foci; and 3, >2 foci. Ballooning was classified as 0, none; 1, few balloon cells; and 2, many balloon cells. In addition, fibrosis staging was defined as 0, none; 1, perisinusoidal and/or pericentral; 2, incomplete central/central bridging fibrosis; 3, complete central/central bridging fibrosis; and 4, definite cirrhosis. NAS was calculated for each liver biopsy based on the sum of scores for steatosis, inflammation and ballooning.

Quantitative analysis of collagen in Sirius Red-stained liver sections was performed using imaging analysis software (ImageJ software (http://imagej.nih.gov)). Briefly, paraffin sections of 20 μm thickness were stained in 0.1% Sirius red in saturated picric acid. The red-stained area (μm^2) was measured in five consecutive fields (40×). Fibrotic area percentage was calculated relative to the total area examined.

2.4. Isolation and culture of hepatocytes

Hepatocytes were isolated from non-fasting male Wt and hCOX-2-Tg mice by perfusion through the inferior cava vein with Hank's balanced salt solution (HBSS) (Gibco), 1 mM HEPES pH 7.4, 0.2 mM EGTA and William's E medium (Sigma) with 0.8 mg/ml collagenase type 1 (Worthington, Biochemical Corporation, USA) [2]. After filtering through a cell strainer (100 μm) and centrifugation at 70 *g*, 4 °C

for 5 min, cells were resuspended in the following attachment cultured medium: DMEM/F12, 20 mM HEPES pH 7.4, 0.05% $NaHCO_3$, 5 mM glucose, 10% FBS (Sigma), 5 mg/ml BSA, 100 U/ml penicillin, 100 μg/ml streptomycin and 50 μg/ml gentamicin, and purified by density gradient centrifugation using a isotonic solution of Percoll (GE Healthcare Bio-Sciences AB, Uppsala, Sweden). Cells were plated in 6 multiwell dishes at a density of 500,000 cells/well in attachment cultured medium with 10% FBS. Cell viability was checked by Trypan blue exclusion. Cells were serum starved at 2% FBS for 4 h and further treated with 2 ng/ml TGF-β1, 5 μM PGE_2 or 5 μM DFU overnight.

2.5. Isolation of Kupffer cells

For Kupffer cells (KC) isolation, the supernatant from the first centrifugation of the hepatocyte isolation protocol was collected and centrifuged twice at 50 *g* for 5 min to discard the pellet with remaining hepatocytes, as described previously [24]. Briefly, the latest supernatant was centrifuged at 500 *g* for 5 min at 4 °C and the pellet containing the KC was resuspended in the attachment culture medium. Cells were mixed by inversion with 50% Percoll and centrifuged at 1059 *g* for 30 min without acceleration or brake at room temperature. Finally, KC pellet was washed with PBS, centrifuged twice at 500 *g* for 10 min at 4 °C to wash out the residual Percoll solution and cells were resuspended directly in TRIzol reagent (Invitrogen, Carlsbad, CA, USA) for further mRNA analysis.

2.6. Isolation and culture of hepatic stellate cells (HSC)

The isolation of HSCs from mice livers was performed as described [25] and can be divided into: *In situ* pronase (0.4 mg/ml) in perfusion solution/collagenase (0.8 mg/ml, increasing 1.5-fold after CCl_4 treatment) in William's E medium of mouse liver; subsequent *in vitro* digestion; and density gradient-based separation of HSCs from other hepatic cell populations. Briefly, after the *in situ* digestion, the liver was carefully removed and minced under sterile conditions. The minced liver was further digested *in vitro* with pre-warmed pronase (0.4 mg/ml)/collagenase (0.8 mg/ml)/DNase I (0.1 mg/ml)/HEPES (10 mM) in HBSS pH 7.3 solution. Then, the liver cell suspension was filtered through a 100 μm cell strainer to eliminate undigested tissue remnants and centrifuged at 600 *g* for 10 min at 4 °C. The pellet of non-parenchymal cells was resuspended in GBSS (Sigma) and purified by density gradient centrifugation using 14% Nycodenz (Sigma). HSC cells were collected from the diffuse white interfase layer and centrifuged in PBS/0.3% BSA at 600 *g* for 5 min at 4 °C. Cells were resuspended directly in TRIzol reagent (Invitrogen) for further mRNA analysis or were plated in 12 multiwell dishes (Corning, New York, USA) with DMEM, 20% FBS and 100 U/ml penicillin, 100 μg/ml streptomycin and 50 μg/ml gentamicin. Cells were cultured by 0, 1 and 3 days.

2.7. Isolation of hepatic non-parenchymal cells (NPCs) for flow cytometry analysis

Hepatic non-parenchymal cells were isolated as described previously [26]. Briefly, liver tissue was excised in $HBSS^{-/-}$ at RT, mashed through a cell strainer (100 μm), centrifuged at 500 *g* for 5 min at RT and the cell pellet resuspended in 36% Percoll-HBSS solution. After centrifugation at 800 *g* for 20 min without brake, erythrocyte lysis was performed for 10 min at RT in 139 mM NH_4Cl, 19 mM Tris–HCl pH 7.2 solution, washed the pellet twice, and resuspended in 100 μl of PBS.

2.8. Flow cytometry

NPC cells (0.3–0.5 × 10^6 cells/test) were incubated for 20 min at RT in the dark with the following antibodies (5 μg/ml): CD11b-Mac1-PECy7 (rat IgG2bk, anti-mouse eBioscience, San Diego CA, USA), CD45-FITC (rat IgG, Beckman), *F*4/80-PE (ratIgG2ak, eBioscience), Ly6C-FITC (rat IgMk, anti-mouse, Pharmingen, San José, CA, USA) and CCR2-APC (ratIgG2B, R&DSystems, Minneapolis, MN, USA) or their corresponding isotype controls. After three washes, Perfect-Count microspheres (Cytognos, Salamanca, Spain) were added to quantify the exact number of cells. Flow cytometry analysis was performed using Cytomics FC500 with the CXP program. In Supplementary Fig. 1 is shown the efficiency of isolation of immune cell population in RCD and MCD groups.

2.9. Hepatic stellate cell lines cultures

The LX-2 cell line, a spontaneously immortalized human hepatic stellate cell, was purchased from (Millipore, Billerica, MA, SCC064) and recently authenticated using Promega's StemElite™ ID System in the Genomics Core facility of the IIB. LX-2 cells were maintained in EmbryoMAX medium (Millipore, Billerica, MA, USA) supplemented with glutamine and 2% foetal bovine serum (Sigma). Cells were maintained in Dulbecco's culture medium (Gibco), supplemented with 5% FBS, in a humidified atmosphere with 5% CO_2. For the activation experiments, cells (4 × 10^5/well) were seeded into six-well culture plates starving, treated with 5 μM PGE_2 overnight and then treated whit 2 ng/ml TGF-β1 for 6 h.

2.10. Determination of metabolites, cytokines and hormones

PGE_2 was determined in liver tissue by specific immunoassay (Arbor Assays, Ann Arbor, MI, USA). Blood glucose levels were measured with an Accu-Check Glucometer (Roche). Serum ALT activity was determined using Reflotron strips (Roche Diagnostics, Barcelona, Spain), accordingly with the manufacturer's instructions. Triglycerides, cholesterol and HDL were determined in plasma by enzymatic methods with specific kits from BioSystems (Wako Chemicals GmbH, Neuss, Germany). Plasma cytokine levels were assessed by Luminex analysis (Luminex 100IS Multiparametric Analyzer). To quantify collagen, hepatic hydroxyproline content was assayed according to the manufacturer's instructions by a hydroxyproline kit (Hydroxyproline Assay Kit, Sigma). Caspase-3 and 8 activities were determined by Caspase-3/8 Fluorogenic Substrate (BD Pharmingen). The protease activity is represented by fluorescence arbitrary units. Protein levels were determined using the Bradford reagent (Bio-Rad) [27].

2.11. Measurement of intracellular redox state

The oxidation-sensitive fluorescent probes 2′,7′-dichlorodihydrofluorescein diacetate (H_2DCFDA) (Invitrogen, Carlsbad, CA, USA) was used *in vitro* to analyze the intracellular redox status [28]. After treatment and at the indicated times, cells were incubated with 5 μM H_2DCFDA (30 min, 37 °C), washed and lysed with a buffer containing: 25 mM HEPES pH 7.5, 60 mM NaCl, 1.5 mM $MgCl_2$, 0.2 mM EDTA and 0.1% Triton X-100 (10 min, 4 °C) and transferred in duplicate into 96-well plate. Fluorescence was measured in a Microplate Fluorescence Reader and corrected by protein content. Lipid peroxidation (LPO) levels were determined as indirect measurements of ROS production. The amount of aldehyde products generated by LPO was quantified *ex vivo* in liver tissue by the TBA reaction according to the method of Ohkawa et al. [29]. Liver tissue (30 mg) were homogenized with 300 μl of 0.15 M KCl and 50 μl of liver homogenate were incubated for 60 min at 95 °C with 0.3% TBA pH 3–3.5, 0.5% SDS and 7.5% acetic acid. The mixture was centrifuged at 4000 *g* for 10 min. The amount of TBA reactants (TBARS) was expressed in terms of MDA using 1,1,3,3-tetramethoxypropane as a standard (nmol MDA/mg protein) [30]. Total (GSHt) and oxidized glutathione (GSSG) were determined in total liver homogenates according to the protocol described by Tietze [31] with slight modifications. Briefly, intracellular GSH and GSSG contents were determined according to

the glutathione reductase–DTNB recycling assay as described previously [32]. Liver lysate was subsequently precipitated by adding 5-sulfosalicylic acid (SSA) and removed by centrifugation. The resulting supernatant was collected and assayed for total GSH and GSSG. To determine GSSG level of the lysate, first, 2-vinylpyridine was added and kept at 37 °C for 1 h to derive GSH.

2.12. RNA isolation

Total RNA of liver and cell samples was extracted by using TRIzol reagent. Total RNA (1 μg) was reverse transcribed using a Transcriptor First Strand cDNA Synthesis Kit following the manufacturer's indications (Roche).

2.13. Quantitative real-time PCR analysis

qPCR was performed with a MyiQ Real-Time PCR System (Bio-Rad) sequence detector using the SsoFast EvaGreen Polymerase method (Bio-Rad) and d(N)6 random hexamer with the primers described in Supplementary Table I. Specific primers were purchased from Invitrogen. PCR thermocycling parameters were 95 °C for 30 s, 40 cycles of 95 °C for 5 s, and 60 °C for 10 s. Each sample was run in triplicate and was normalized to 36b4 RNA. The replicates were then averaged, and fold induction was determined in a ΔΔCt based fold-change calculations.

2.14. Western blot analysis

Extracts from tissue samples (50–100 mg) or cells ($2–3 \times 10^6$) were obtained as previously described [21]. Nuclear and cytosolic extracts were isolated from 100 mg of liver tissue with 0.3 M sucrose solution. The homogenate was centrifuged at 1000 *g* at 4 °C for 10 min to separate the cytosolic fraction (supernatant) and nuclear fraction (pellet). The supernatant was centrifuged 3 times at 18,600 *g* at 4 °C for 20 min, and collected in a new tube. The pellet was washed 4 times with 0.3 M sucrose solution, and centrifuged at 1000 *g* at 4 °C for 10 min. After, the pellet was resuspended in RIPA and shaked at 4 °C for 1 h. The nuclear extract was obtained through centrifugation at 8000 *g* at 4 °C for 15 min. Finally, the total protein was measured as previously described [21].

For Western blot analysis, whole-cell extracts were boiled for 5 min in Laemmli sample buffer, and equal amounts of protein (20–30 μg) were separated by 10–15% SDS-polyacrylamide electrophoresis gel (SDS-PAGE). The relative amounts of each protein were determined with the polyclonal or monoclonal antibodies described in Supplementary Table II. After incubation with the corresponding anti-rabbit or anti-mouse horseradish peroxidase conjugated secondary antibody, blots were developed by the ECL protocol (GE Healthcare Life Sciences, Pittsburgh, PA, USA). Target protein band densities were normalized with GAPDH. The blots were revealed, and different exposition times were performed for each blot with a charged coupling device camera in a luminescent image analyzer (LAS 500, GE) to ensure the linearity of the band intensities. Densitometric analysis of the bands was carried out using ImageJ software (http://imagej.nih.gov) and expressed in arbitrary units.

2.15. Data analysis

Data are expressed as means ± S.E. Statistical significance was estimated using Student 2-tailed *t*-test to evaluate the differences between treated and untreated mice within a single genotype and between genotypes. Analysis was performed by using the statistical software GraphPad Prism 5. A $p < 0.05$ was considered statistically significant.

3. Results

3.1. Sustained liver COX-2 expression protects transgenic mice from MCD-induced hepatic steatosis and liver damage

The majority of current NASH mouse models do not fully recapitulate the human condition, however, the MCD diet model is characterized by the rapid appearance of steatosis in 2–4 weeks, inflammation and cell death, which represent the main features of steatohepatitis and replicates NASH histological phenotype [33]. The MCD diet model induces experimental NASH through the assessment of the inflammatory pathway and this model was used to study this stage of the disease [34]. We used our previously described transgenic mice (hCOX-2-Tg) that constitutively express human COX-2 in hepatocytes under the control of the human ApoE promoter and its specific hepatic control region (HCR). The expression of hCOX-2 is only achieved in the hepatocytes of hCOX-2-Tg mice, and is comparable to the physiologic levels reached in the regenerating liver after partial hepatectomy [3,5]. We found levels of PGE_2 >3 fold higher in hCOX-2-Tg compared to Wt mice, even when there is a clear tendency to increase PGE_2 hepatic levels in Wt mice with the MCD diet (Fig. 1A–B). This increase is associated with an induction of endogenous COX-2 expression (data not shown). After 2 and 4 weeks of MCD diet, both Wt and hCOX-2-Tg mice showed a marked decrease in body weight (>30%), and this fact cannot be associated with food intake differences (data not shown). Although no significant differences were found in weight loss between hCOX-2-Tg and Wt mice during the first 2 weeks, from the third week of treatment the decrease on body weight was significantly attenuated in hCOX-2-Tg (Fig. 1C). Administration of MCD diet resulted in a marked elevation of serum ALT, but it was significantly lower in hCOX-2-Tg mice (Fig. 2D). Plasma biochemistry is shown in Supplementary Table III.

To correlate the increase in ALT levels with the histological damage, liver sections were stained with hematoxylin/eosin (H&E) and Masson's trichromic (MTC) and then assessed by an experienced liver pathologist. The MCD diet induced a marked steatosis in both Wt and hCOX-2-Tg mice whereas the hepatic fat amount was significantly lower in hCOX-2-Tg mice at 4 weeks (Fig. 2A–B). A significant decrease in the inflammation and ballooning (a characteristic form of hepatocellular injury in steatohepatitis) scores was observed at 4 weeks in hCOX-2-Tg (Fig. 2C-D). No MTC staining was observed neither in Wt or hCOX-2-Tg liver after MCD. Likewise, NAFLD activity score was significantly lower in hCOX-2-Tg mice fed MCD diet during 4 weeks than in Wt litter-mates. To note, MCD-hCOX-2-Tg mice recover faster to pre-treatment situation after feeding a RCD diet. Body weight (Fig. 3A) recovery was significantly higher in hCOX-2-Tg. Similar results were obtained in plasma ALT levels (Fig. 3B) associated with a significantly decrease in NAFLD activity score (Fig. 3C–D), showing not only that constitutive hepatic COX-2 expression attenuated the damage under MCD but also lead to a faster recuperation.

3.2. COX-2 expression reduced hepatic inflammation in a diet-induced NASH model

In NASH dietary model, steatosis and elevated serum ALT levels are followed by inflammation [35]. As is shown in Fig. 2C, MCD diet for 4 weeks induced moderate to severe lobular inflammation in Wt mice liver, whilst it was mild to moderate in hCOX-2-Tg mice. Our previous data [5,20] showed lower levels of inflammatory markers in hCOX-2-Tg mice after liver injury. After 4 weeks of MCD diet, the plasmatic levels of IL1-β, IL-6, TNF-α and MCP-1 were increased by MCD especially in Wt mice *vs.* hCOX-2-Tg counterparts (Fig. 4A). Chemokines play pivotal roles in the recruitment of immune cells at sites of inflammation [36]. To gain insight into the process, we isolated non-parenchymal cells (NPCs) from liver and analyzed the monocyte recruitment in mice fed the MCD diet for 4 weeks. Similar number of $CD45^+$ cells (leukocyte common antigen) was detected in Wt and hCOX-2-Tg mice livers

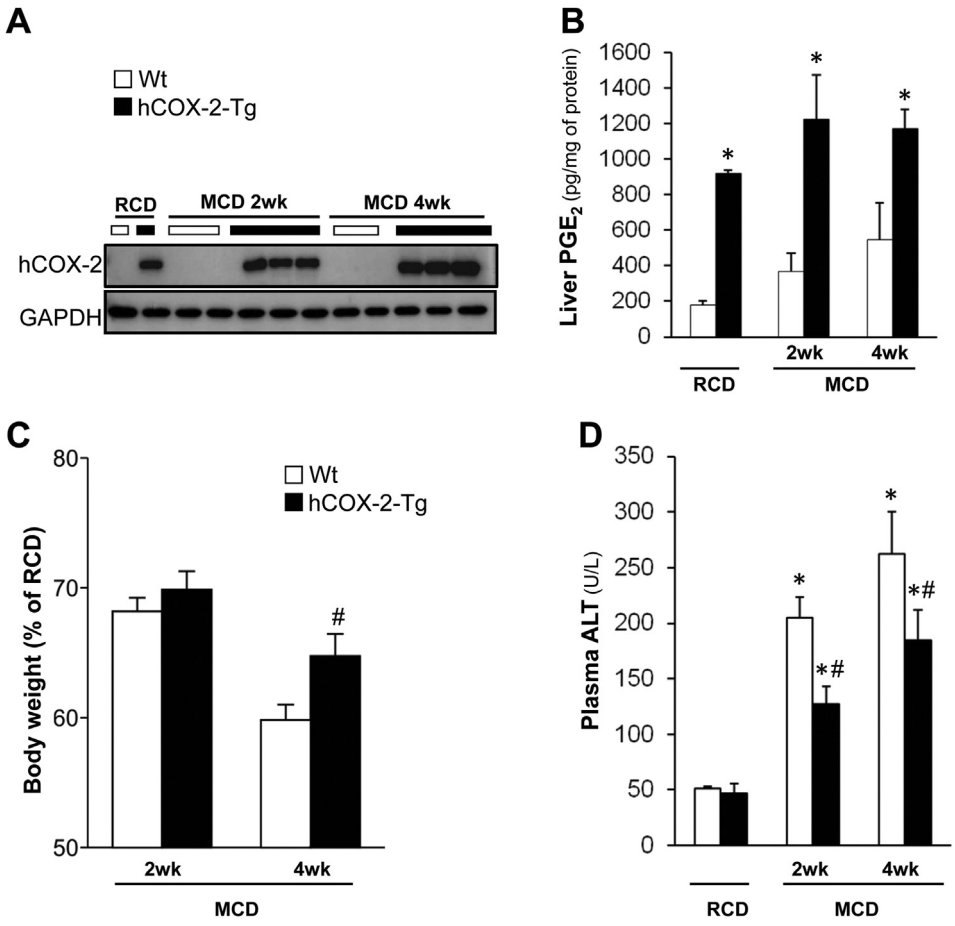

Fig. 1. hCOX-2-Tg mice are protected against MCD-induced liver damage. Wt and hCOX-2-Tg mice were fed MCD *ad libitum* for 2 and 4 weeks. (*A*) Human COX-2 protein was only detected in hCOX-2-Tg mice liver extracts and consistently, PGE_2 levels measured by EIA (*B*) were three fold higher *vs.* Wt mice. (*C*) Body weight of Wt and hCOX-2-Tg mice fed MCD expressed as percentage of basal body weight. (*D*) Plasma levels of ALT in Wt and hCOX-2-Tg mice. Data are expressed as means ± S.E. ($n = 5$–6 per group). $^*p < 0.05$ *vs.* Wt-RCD; $\#p < 0.05$ *vs.* Wt-MCD.

under RCD; but MCD diet produced a 5 fold increase in the number of $CD45^+$ cells in the livers from Wt mice *vs.* a 3 fold increase in hCOX-2-Tg mice (Fig. 4B and Supplementary Fig. 1). Analysis of the hepatic recruited monocytes revealed that following MCD diet there was an increased number of $F4/80^+$ $CD11b^+$ cells (macrophages) in Wt livers (Fig. 4C), whereas there were no significant increase in the hCOX-2-Tg mice, showing an attenuated inflammatory response. As shown in Fig. 4D, when we analyzed MCP-1-associated macrophage recruitment by evaluating the CCR2 levels, the number of CCR2-expressing cells was higher in MCD diet fed Wt mice. Also the number of cells that express Ly6C (inflammatory monocytes), a marker for bone marrow (BM)-derived circulating peripheral blood monocytes [37], was significantly increased in the Wt-MCD livers, whereas this effect was attenuated in hCOX-2-Tg mice (Fig. 4E). These results agree with previous reports suggesting that infiltrated hepatic macrophages express CCR2 inflammatory phenotypes in diet-induced NASH model and HFD/obese mice [38,39]. Concordantly, in Fig. 4F and G we show that hepatic COX-2 expression attenuates MCD-induced increase of pro-inflammatory genes in total liver and specifically in isolated Kupffer cells, respectively.

3.3. Constitutive hepatocyte COX-2 expression leads to decreased apoptosis and oxidative stress

Previously, we reported that hepatocyte apoptosis was increased in NASH [9], and clearly established the anti-apoptotic role of hepatic COX-2 expression [21,40]. To further explore the protective effect of COX-2 expression, caspases activities and some key apoptotic/antiapoptotic protein levels were measured. As shown in Fig. 5A, both caspase-3 and -8 activities increased only in MCD-Wt mice at 4 weeks. Consistent with this, an important increase in the Bax/Bcl-x_L ratio was found only in MCD-Wt mice. Even more, the attenuation found in hCOX-2-Tg mice livers could be explained in part by an increase in the anti-apoptotic protein Mcl-1 (Fig. 5B). Steatohepatitis is associated with the generation of reactive oxygen species and other oxidative stress-related compounds. Lipid peroxidation (LPO) was determined by the reaction of thiobarbituric acid (TBA) with malondialdehyde (MDA). LPO increased by MCD diet in both genotypes, but in a lesser extent in hCOX-2-Tg mice livers (Fig. 5C). The ratio of oxidized glutathione/total gluthatione, evaluated as an intracellular redox status marker, was significantly higher only in Wt mice after 4 weeks of MCD diet (Fig. 5C). The products derived from lipid-peroxidation can mediate inflammatory recruitment by activating nuclear factor-κB (NF-κB). Also, it is known that NF-κB is activated in MCD-diet-induced steatohepatitis occurring in both hepatocytes and non-parenchymal cell fraction [17,41]. To know whether NF-κB is involved in the regulation of inflammation in our model, nuclear p65 and cytosolic IκBα protein levels were measured in Wt and hCOX-2-Tg liver after MCD. As shown in Fig. 5D, an important increase in nuclear p65 and phosphorylated cytosolic IκBα protein levels indicating a NF-κB pathway activation, was found in MCD-Wt mice whereas this activation was attenuated in MCD-hCOX-2-Tg mice.

3.4. PGE_2 protects isolated primary hepatocytes against TGF-β1-dependent apoptosis and oxidative stress

It has been described that TGF-β1 signaling in hepatocytes participates in steatohepatitis through regulation of cell death [42]. As

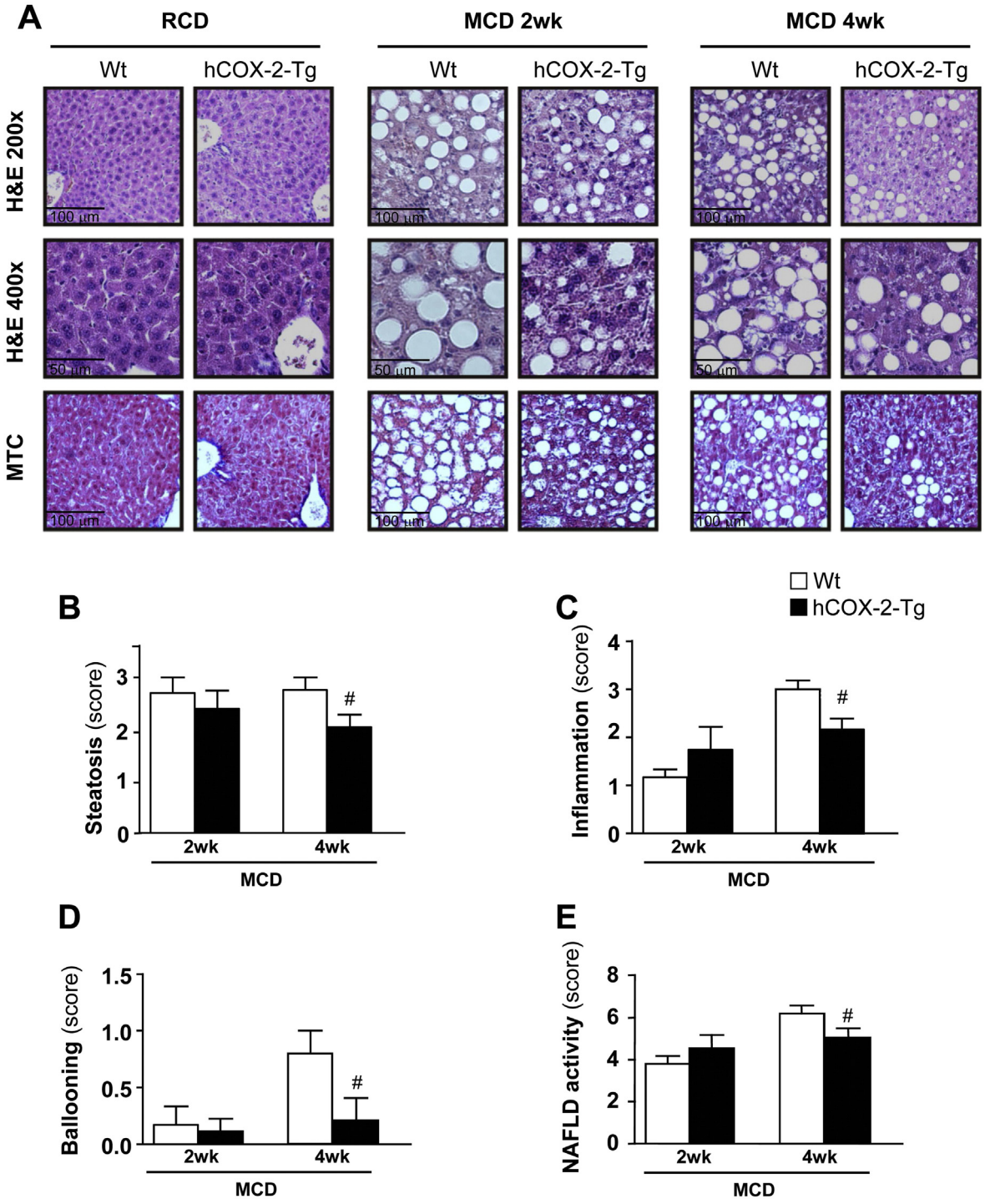

Fig. 2. COX-2 transgenic mice are protected against MCD-induced hepatic steatosis, inflammation and ballooning. (*A*) Representative images of hematoxylin/eosin (H&E) and Masson's trichromic (MTC) stained liver paraffin-embedded sections from Wt and hCOX-2-Tg mice fed RCD or MCD for 2 and 4 weeks. (*B*) Quantification of steatosis (*C*) Inflammation (*D*) Balloning and (*E*) NAFLD activity score. Data are expressed as means ± S.E. ($n = 5$–6 per group). #$p < 0.05$ *vs.* Wt-MCD 4 wk.

shown in Fig. 6A–C, TGF-β1 induced caspase-3 activity and leads to increased Bax/Bcl-x_L ratio in isolated hepatocytes from Wt mice. However, TGF-β1 did not induce apoptosis in hepatocytes from hCOX-2-Tg mice. Furthermore, when Wt hepatocytes were co-treated with TGF-β1 and PGE_2, apoptosis was decreased and, conversely, when hCOX-2-Tg hepatocytes were treated with DFU, a COX-2 selective inhibitor; there was an increase in caspase-3 activity and in the Bax/Bcl-x_L ratio, indicating the specificity of COX-2-dependent prostaglandins in the modulation of TGF-β1-induced apoptosis. The oxidation-sensitive fluorescent probe DCFH was used to analyse the intracellular redox status. As shown in Fig. 6D, TGF-β1 increased DCFH fluorescence only in Wt hepatocytes. PGE_2 treatment reversed this effect and pretreatment with DFU increased DCFH fluorescence in hCOX-2-Tg hepatocytes. Induction of mRNA levels of antioxidant genes such as *Cat*, cytosolic *Sod1*, mitochondrial *Sod 2* and *Grs* (Supplementary Table IV) seems to mediate this effect in hCOX-2-Tg hepatocytes.

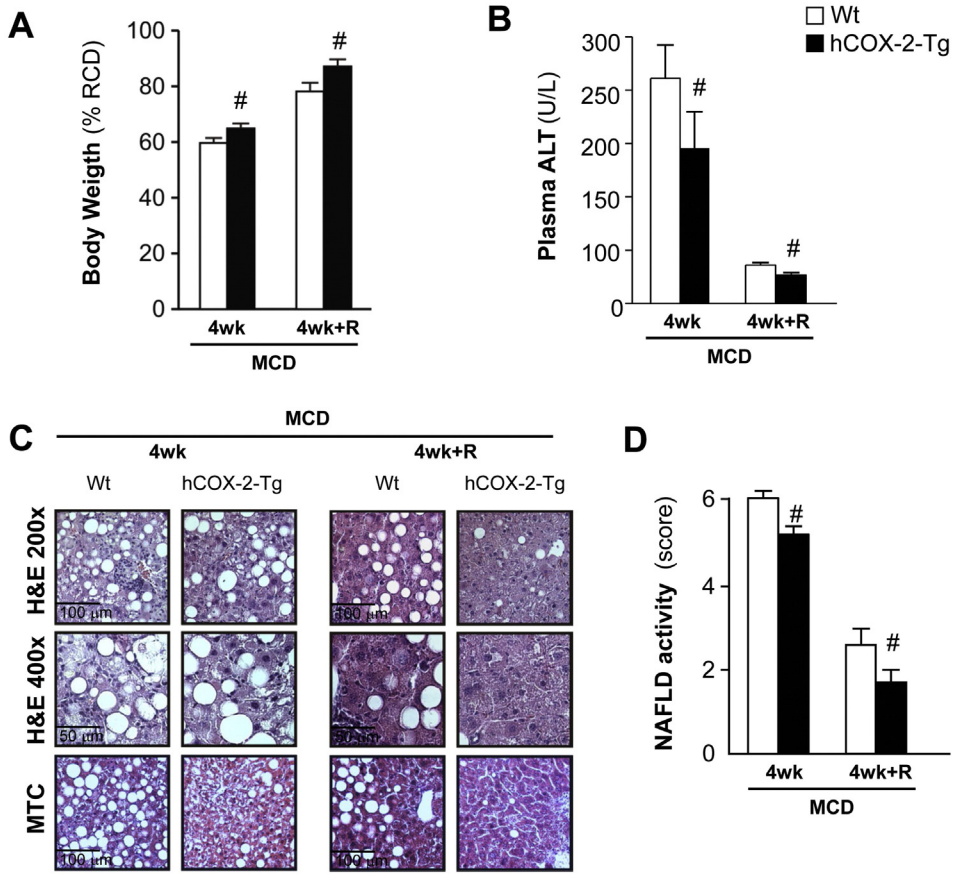

Fig. 3. MCD-COX-2-Tg mice recover to pre-treatment situation after feeding with RCD diet. Diet recovery models (group R-Wt and R-hCOX-2-Tg) were established by switching the Wt and hCOX-2-Tg mice fed a MCD for 4 weeks to the control, RCD, diet for 5 days. (*A*) Body weight of Wt and hCOX-2-Tg mice expressed as percentage of basal body weight. (*B*) Plasma levels of ALT in Wt and hCOX-2-Tg mice. (*C*) Representative images of stained with hematoxylin/eosin (H&E) and Masson's Trichrome (MTC) liver paraffin-embedded sections from Wt and hCOX-2-Tg mice. (*D*) Quantification of NAFLD activity score. Data are expressed as means ± S.E. for 6 mice of each experimental group. #$p < 0.05$ *vs.* Wt-MCD or Wt-MCD + R.

3.5. Hepatocyte COX-2 expression attenuates pro-fibrogenic markers in a CCl_4-induced liver fibrosis model

To investigate the role of hepatocyte COX-2 expression on fibrosis, we injected CCl_4 in Wt and hCOX-2-Tg mice twice a week for 9 weeks. Liver sections were stained with H&E, MTC and Picro Sirius Red to evaluate fibrosis stage and to quantify the size of the fibrotic area. We found a delayed progression in fibrosis stage in hCOX-2-Tg mice (Fig. 7 A–B). It is known that TGF-β signaling in hepatocytes participates in steatohepatitis and fibrosis through regulation of cell death *via* phosphorylation and translocation of SMAD2/3 [42]. As shown in Fig. 7C and D, an important increase in phosphorylated SMAD2/3 was found in Wt mice after CCl_4 whereas the signaling was attenuated in hCOX-2-Tg mice. The reduced fibrosis seen in hCOX-2-Tg mice livers correlated with both a lower collagen 1a1 expression and hepatic hydroxyproline content (Fig. 7C and E). We next analyzed the activation of the pro-fibrogenic markers, desmin, α-SMA and vimentin and observed a significant decrease in all of them in hCOX-2-Tg mice *vs.* the Wt mice (Fig. 7C and F).

Concordantly, hepatic mRNA levels of *desmin*, *α-SMA* and *Col1a1* were lower in hCOX-2-Tg livers after CCl_4 treatment (Supplementary Fig. *2*). Also, hCOX-2-Tg livers showed lesser CCl_4-induced levels of PDGF-B and its receptor, known contributors to fibrogenesis [43]. In addition, COX-2 expression was able to induce mRNA expression of HGF, a potent suppressor of liver fibrosis [44] (Supplementary Fig. *2*). In summary, hepatic expression of COX-2 attenuated the induction of fibrogenic markers in a CCl_4-induced liver injury model.

3.6. Prostanoids derived from COX-2 inhibit hepatic stellate cell activation both in vivo and in vitro

The reduced collagen deposition seen in hCOX-2-Tg mice livers after CCl_4 treatment prompted us to investigate a possible different activation of HSC cells in Wt and Tg mice in response to prostaglandins produced by hepatocytes (Hep), since hCOX-2 expression was only detectable in isolated Hep and not in HSC (Fig. 8A). mRNA expression level of *Col1a1* and *α-SMA* in HSCs isolated from hCOX-2-Tg mice after 9 weeks of CCl_4 treatment showed lesser increase compared to Wt livers (Fig. 8B), suggesting that the hepatocyte expression of COX-2 prevents HSC activation *in vivo*. Then, we tested the specific role of PGE_2 on HSC activation *in vitro*, and found that Col1a1 and α-SMA levels in cell extracts from human HSC line (LX-2) induced by TGF-β1 were reverted by the pre-treatment with PGE_2, pointing out its anti-fibrotic action (Fig. 8C). Even more, to determine the possible signaling pathways related with COX-2 and involved in α-SMA expression, LX-2 cells were treated with pharmacological inhibitors of phosphatidylinositol-3-kinase (PI3K) (LY294002), protein kinase C (PKC) (Gö6983), PKA (4-cyano-3-methyl-isoquinoline, CMI), p38 mitogen-activated protein kinase (BRIB796), mitogen activated protein kinase/extracellular signal-regulated kinase (MEK/ERK) (PD98059), and NF-κB (BAY11-7085), as well as antagonist of EP receptors. LX-2 cells express mRNAs of the four EP receptors (data not shown). As shown in Fig. 8D, most of the inhibitors reverse the decrease in α-SMA protein levels produced by PGE_2, implicating a complex process where PKC, PKA, p38, MEK/ERK and NF-κB signaling pathways are involved.

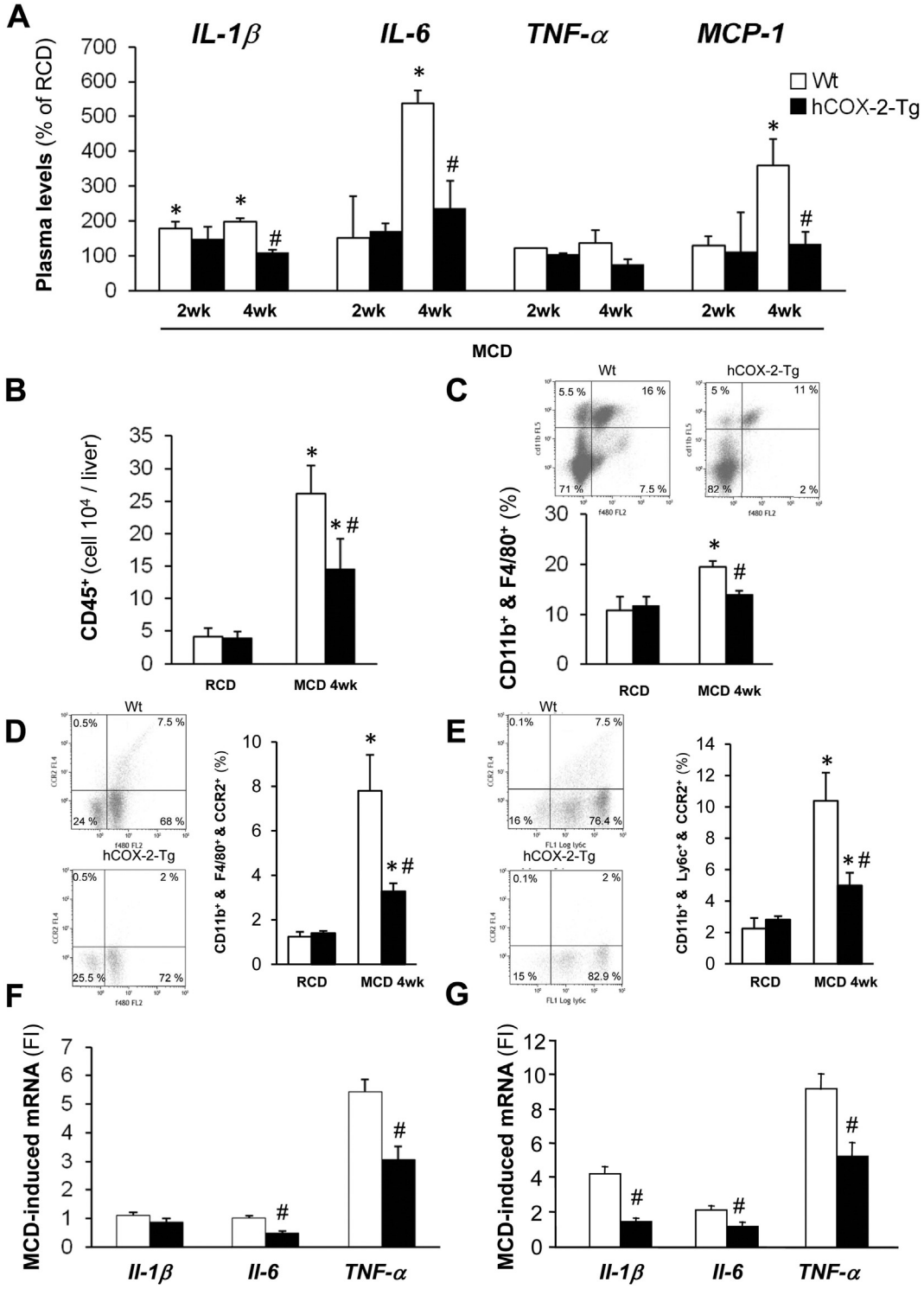

Fig. 4. Analysis of pro-inflammatory cytokines and hepatic macrophage recruitment in Wt and hCOX-2-Tg mice under MCD diet. (*A*) Plasmatic levels of IL-6, IL-1β, TNF-α and MCP-1 were assessed by Luminex analysis. Values are represented as fold increase relative to Wt-RCD. (*B*) Analysis of CD45$^+$ isolated liver cells (***C***). *F*4/80$^+$ and CD11b$^+$ cells from the CD45$^+$ gated cells in (*B*). (*D*) CCR2$^+$ cells from *F*4/80$^+$CD11b$^+$ and (*E*) from CD11b$^+$Ly6C$^+$ cells. Data are expressed as means ± S.E. ($n = 5$–6 per group). *$p < 0.05$ *vs.* Wt-RCD; #$p < 0.05$ *vs.* Wt-4 wk MCD. mRNA MCD fold induced (FI) levels of pro-inflammatory markers in liver (*F*) and in isolated Kupffer cells (*G*). Data are expressed as means ± S.E. ($n = 4$ per group). #$p < 0.05$ *vs.* Wt-4 wk MCD.

Moreover, the data suggest that PGE_2 exerts its effects through EP2 and EP4 receptors (Fig. 8 E).

4. Discussion

The impact of PGE_2 on the development of NASH and hepatic fibrosis is a matter of controversy. Some studies in animal models suggest that COX-2-derived PGs favor the development of steatohepatitis and fibrosis in view of the beneficial effects after selective inhibitors (COXIBs) treatment [15,16], whilst others describe the opposite and provide evidence that PGE_2 suppresses fibrogenesis in HSC and the progression of steatohepatitis [14,18,19]. Even more, Yu et al. by using liver COX-2 transgenic mice, but in a different genetic background than ours, reported that COX-2 does not appear to mediate the development of liver

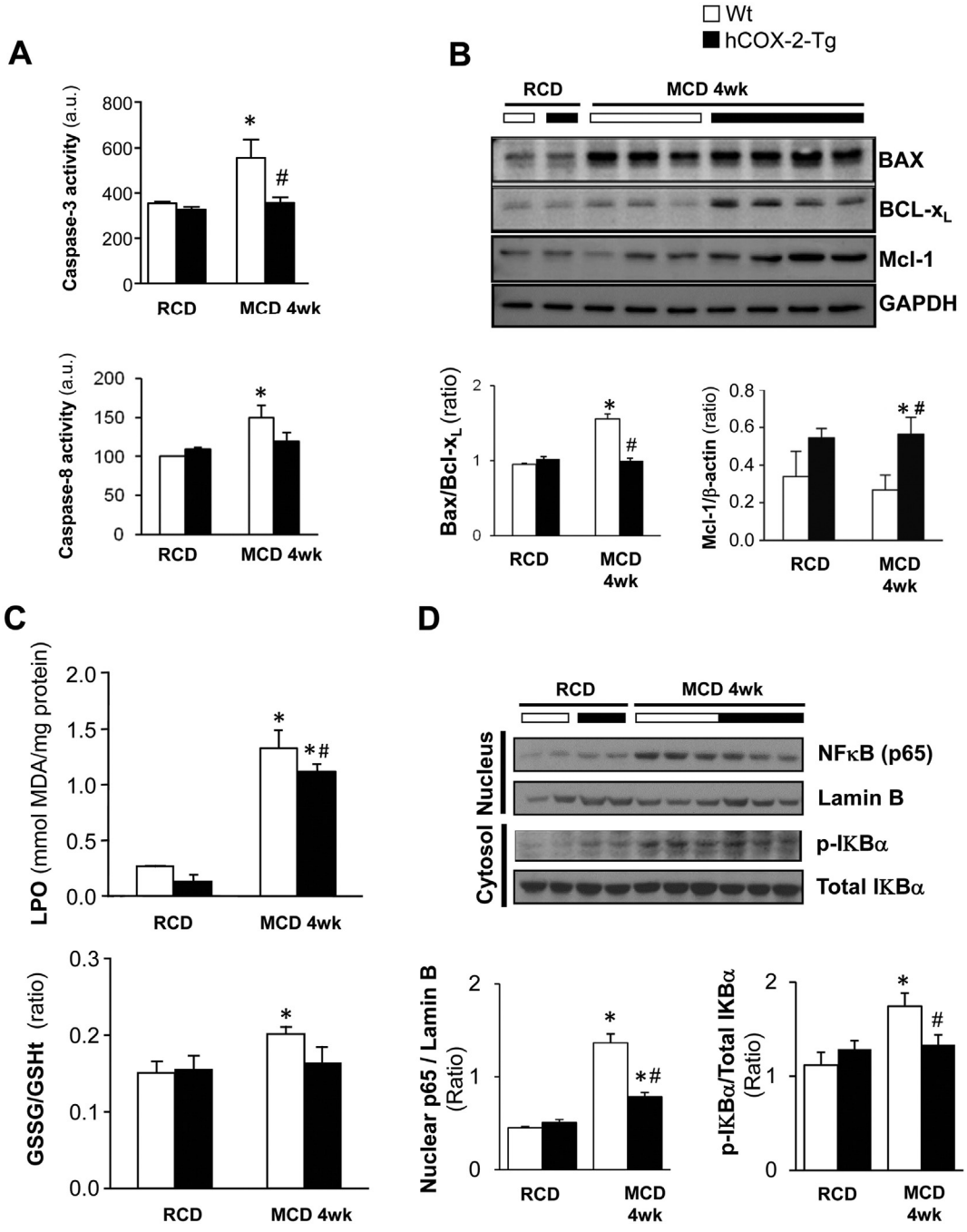

Fig. 5. COX-2 expression leads to decreased apoptosis and oxidative stress. (*A*) Caspase-3 and Caspase-8 activity in liver extracts from Wt and hCOX-2-Tg mice fed RCD and MCD for 4 weeks. (*B*) Representative Western blots and densitometric analysis of Bax, Bcl-x_L and Mcl-1 protein levels. (*C*) Lipid peroxidation determined by the reaction of thiobarbituric acid (TBA) with malondialdehyde (MDA) in liver homogenates and Oxidized glutathione/Total glutathione ratio (GSSG/GSHt) content. (*D*) Representative Western blots and densitometric analysis of p65 and phospho-IκBα protein levels that were analyzed in nuclear and cytosolic liver extracts respectively. Data are expressed as means ± S.E. ($n = 4$–5 per group). $^{*}p < 0.05$ *vs.* Wt-RCD; $\#p < 0.05$ *vs.* Wt-MCD.

fibrosis [45]. Our previous results indicate a protective role for COX-2 in liver injury by several insults [5,21,40] and pointed out COX-2 as a key player in the development of metabolic alterations [20,46]. It was reported that in mice fed the MCD diet, hepatic expression of COX-2 occurred paralleling the development of steatohepatitis [17]. To assess this induction as a possible physiologic early protective response to liver injury, we evaluated the role of sustained hepatic COX-2 expression in a murine model of dietary-induced steatohepatitis and hepatic fibrosis, resembling two different stages of NAFLD progression.

The MCD diet hallmarks include a rapid appearance of steatosis, inflammation and cell death [47]. Under these conditions COX-2 attenuated elevation of serum ALT which correlated to lower scores of key features of NASH on liver biopsies such as steatosis, inflammation and hepatocyte injury. Indeed, steatosis was significantly lower in hCOX-2-Tg mice, resembling the COX-2 anti-steatosis effect on a HFD model [20]. We used MCD dietary model to induce NASH and, after 4 weeks of MCD diet, Wt mice showed moderate to severe lobular inflammation, whilst in hCOX-2-Tg mice this was mild to moderate. Consistent with a previous report [5] constitutive hepatic expression of COX-2 leads to lower plasmatic levels of pro-inflammatory cytokines (*i.e.* IL-1β and IL-6 and MCP-1) after MCD. MCP-1 is a potent chemoattractant mediator, highly expressed in Kupffer cells, and its

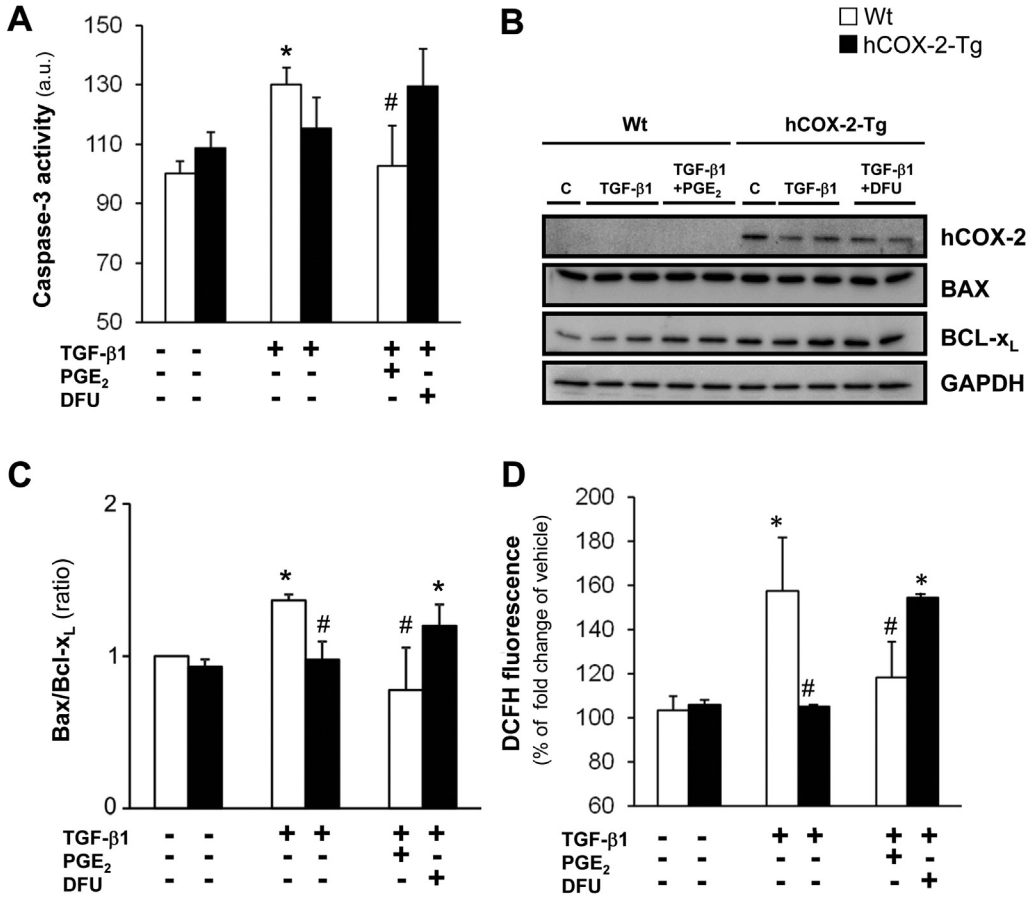

Fig. 6. PGE_2 protects isolated hepatocytes against TGFβ1-dependent apoptosis and oxidative stress. (*A*) Caspase-3 activity in isolated hepatocytes from Wt and hCOX-2-Tg mice after treatment with 5 μM PGE_2, 2 ng/ml TGFβ1 and 5 μM DFU overnight. (*B*) Representative Western blot and (*C*) densitometric analysis of the ratio Bax/Bcl-x_L normalized against GAPDH of primary hepatocytes from Wt and hCOX-2-Tg livers. (*D*) Redox status estimated by DCFH fluorescence. Data for 3 independent experiments. $^*p < 0.05$ *vs.* Wt without treatment; $\#p < 0.05$ *vs.* Wt-TGFβ1 condition.

receptor, the C—C chemokine receptor type 2 (CCR2), is highly expressed in hepatic recruited macrophages compared to resident hepatic macrophages (KCs) [38,39]. Hepatic COX-2 derived PGE_2 could modulate MCP-1 release, as it has proved to be the case in human pulmonary fibroblasts [48]. Recent studies demonstrated that the recruited macrophages predominantly express CCR2 and this inflammatory phenotype promoted liver steatosis and fibrosis [49,50]. Our data also demonstrate a protective effect of continuously hepatic PGE_2 production on the total number of hepatic leukocytes ($CD45^+$). In this regard, as previously reported [38], we found a diet-induced rise in infiltrated hepatic macrophages with inflammatory phenotypes ($Ly6C^+CCR2^+$) in Wt mice but, interestingly, hCOX-2-Tg livers presented an attenuated inflammatory response, including Kupffer cells, with lower levels of pro-inflammatory markers leading to a diminished liver injury. In a recent report, it was suggested a prominent role for hepatocyte caspase-3 activation in NASH-related apoptosis and fibrogenesis that was in part mediated *via* CCR2-dependent infiltration of $Ly6C^+$ macrophages [51]. In this regard, the role of COX-2 dependent PGs by modulating caspase-3 activity is well documented [5,40,52]. Our *in vivo* data support an attenuated inflammatory response, at least in part, by decreasing NF-κB activation derived from MCD diet, an anti-apoptotic effect of COX-2 in the NASH model and an improved antioxidant response to oxidative stress induced by MCD diet.

It is known that TGF-β signaling in hepatocytes promotes steatohepatitis *via* regulation of cell death and lipid metabolism. TGF-β signaling in hepatocytes induces hepatic steatosis, cell damage, inflammatory cell infiltration and fibrosis through Smad activation and ROS production, all conditions contributing to NASH [42]. In agreement with previous data [53], our *in vitro* results by treating Wt and hCOX-2-Tg hepatocytes with TGF-β1 indicate that PGE_2 protects isolated hepatocytes against TGF-β-dependent apoptosis and oxidative stress as deduced by the important decrease of caspase-3 activation and ROS production.

Hepatic fibrosis is the wound-healing response of the liver entailing major alterations in the composition and quantity of the extracellular matrix (ECM). Hepatic stellate cells (HSC) are the key matrix-producing cells in liver and play a central role in hepatic fibrogenesis. Interestingly enough, hepatocyte COX-2 expression delayed fibrosis progression through a decrease in SMAD signaling and significantly decreased the fibrotic area in part by a lesser activation of HSC. These observations are in agreement with previously reported antifibrotic effects of COX-2-derived prostanoids [14,15,54]. Also, the beneficial effects of prostaglandins could be mediated by the induction of anti-fibrotic (HGF) [44] and by down-regulation of pro-fibrotic (PGDFB family members) factors [43]. In this regard, the lesser ECM deposition after CCl_4 treatment found in hCOX-2-Tg livers coincided with diminished HSC activation markers (*i.e.* α-SMA). Indeed, hepatic COX-2 expression prevents HSC activation *in vivo*. Moreover, *in vitro* treatment with PGE_2 counteracts the activation observed in LX-2 human HSC line by TGFβ1, in agreement with previous reports [14,19]. Recently, it was described that in the fibroblast to myofibroblast differentiation process elicited by TGF-β1, PGE_2 was able to reverse the expression of 62% of up-regulated and 50% of the down-regulated genes modulated by TGF-β1, pointing out an anti-TGF-β1 action by PGE_2 [55]. Regarding the mechanism by which PGE2 mediated the attenuation of matrix production by HSC, there are various signaling pathways implicated as well as different

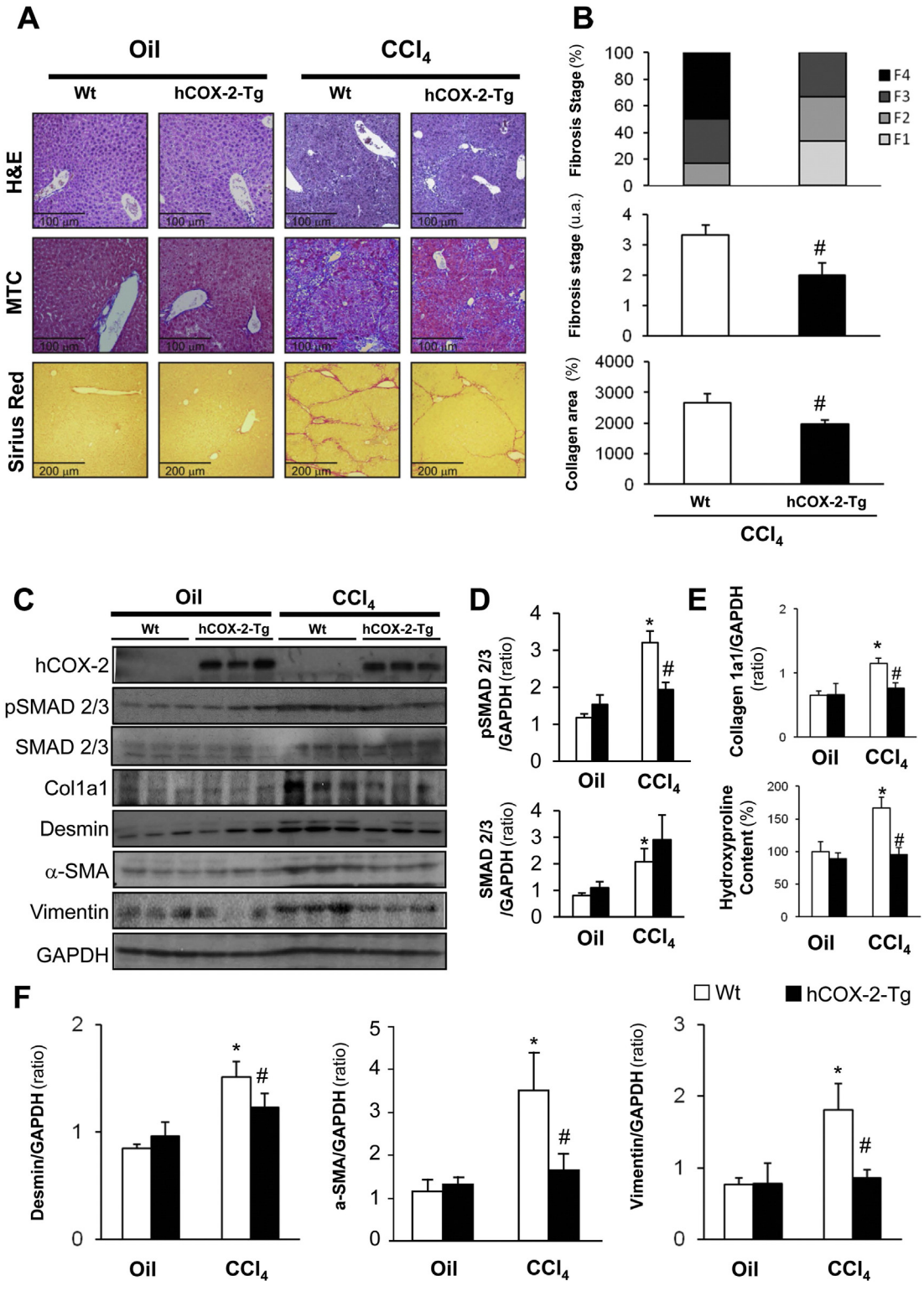

Fig. 7. Hepatocyte COX-2 expression attenuate pro-fibrogenic markers in a chronic CCl_4-induced liver injury model. (*A*) Representative images of hematoxylin/eosin (H&E), Masson's trichromic (MTC) and Picro-Sirius Red stained liver paraffin-embedded sections from Wt and hCOX-2-Tg mice after 9 weeks of CCl_4 treatment. (*B*) Quantification of fibrosis stage (*C*) Representative Western blot and densitometric analysis of (*D*) phospho-SMAD2/3 and total SMAD2/3, (*E*) collagen 1a1 and hepatic hydroxyproline content, (*F*) desmin, α-SMA and vimentin. Data are expressed as means ± S.E. ($n = 6$–8 per group). $^*p < 0.05$ *vs.* Wt-Oil; $\#p < 0.05$ *vs.* Wt-CCl_4.

EP receptors. In agreement with previous data, PGE2 inhibits α-SMA transcription through EP2/cAMP/PKA signaling in human lung fibroblasts [56]. Moreover, PGE2 exerts a suppressive effect on fibrogenesis in pancreatic stellate cells *via* the cAMP pathway and suggest a role of EP2 and EP4 receptors [57]. Our data suggest that PGE_2 exerts its effects through EP2 and EP4 receptors in human LX-2 cells.

As pro-inflammatory mediator, PGE_2 is involved in the pathogenesis of several diseases; since COX inhibitors seem to be effective in reducing some deleterious effects. Accordingly, different *in vivo* models of liver fibrosis [15,16] reported beneficial effects of COXIBs, such as celecoxib. Opposite to this, pro-fibrogenic properties of celecoxib have been reported, worsening the fibrotic process with more HSCs activation [18].

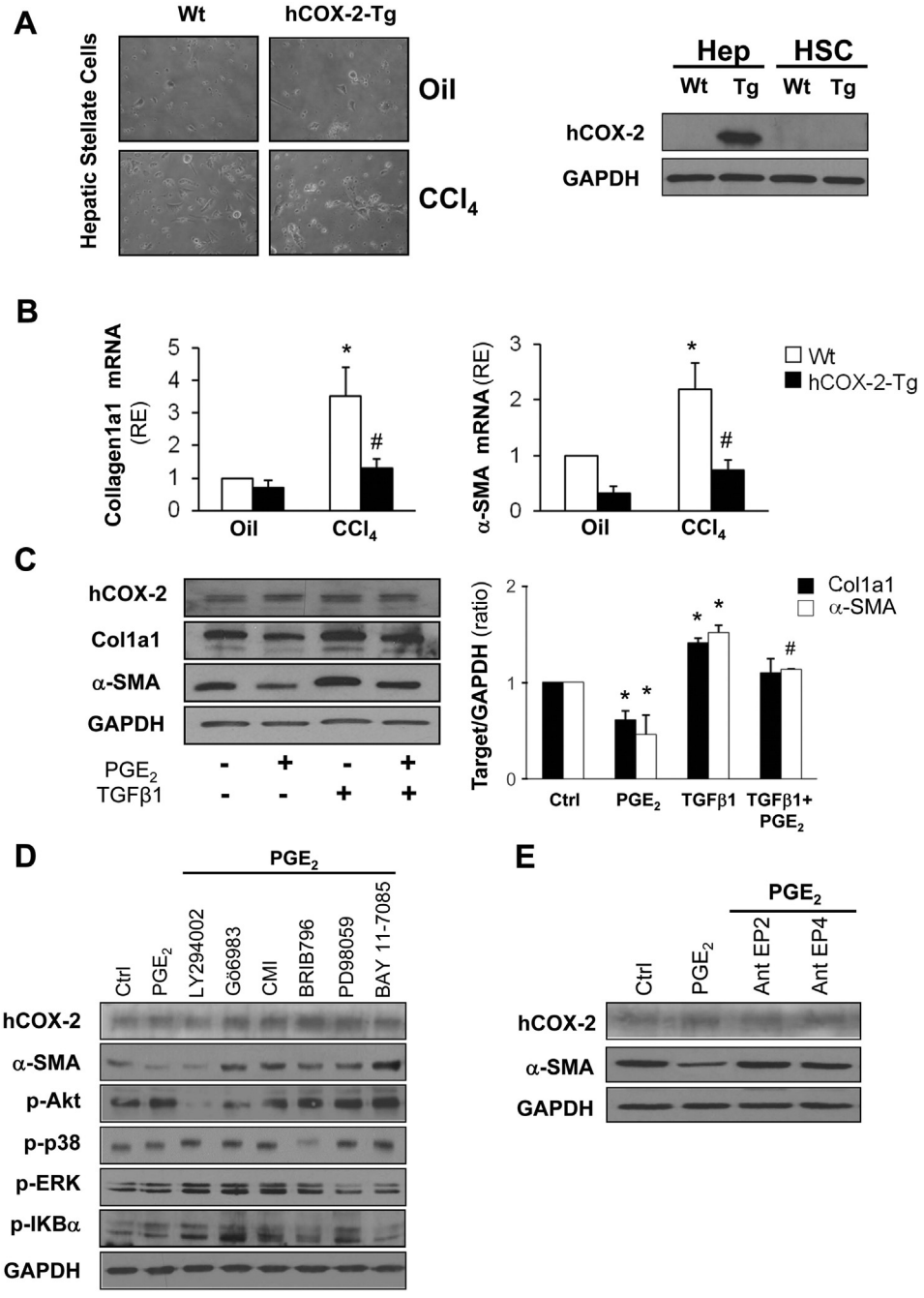

Fig. 8. Hepatic COX-2 expression prevents HSC activation. Role of PGE_2 *in vitro*. (*A*) Microphotography of 3 days cultured HSCs isolated from Wt and hCOX-2-Tg mice after 9 weeks of CCl_4 treatment. hCOX-2 protein levels in hepatocytes (Hep) and HSC cells from Wt and hCOX-2-Tg mice (*B*) mRNA expression of *Col1a1* and *α-SMA* in HSCs. Data are expressed as means ± S.E. for 10–12 mice of each experimental group. *$p < 0.05$ *vs.* Wt-Oil; #$p < 0.05$ *vs.* Wt-CCl_4·(*C*) Representative Western blot and densitometric analysis of Col1a1 and α-SMA/GAPDH ratios in cell extract from human LX-2 cell line treated with 5 μM PGE_2 overnight and/or 2 ng/ml TGF-β1 for 6 h. (*D*) LX-2 cells were serum starved for 6 h prior to treatment with 5 μM PGE_2 and different pharmacological inhibitors for 12 h (20 μM LY294002, 1 μM Gö6983, 0.4 μM CMI, 0.5 μM BRIB796, 50 μM PD98059, and 10 μM BAY11–7085) and EP receptor antagonist (1 μM Ant EP2 (TG4–155) and 25 μM Ant EP4 (GW627368X)). Protein levels were analyzed by Western blot. Data for 3 independent experiments. *$p < 0.05$ *vs.* Ctrl; #$p < 0.05$ *vs.* TGF-β1.

Again, controversy exists since the *in vitro* effects of celecoxib appear to be COX-2-independent [58]. Specifically, it has been demonstrated that celecoxib induces apoptosis of human and rat-derived HSCs [16] but, interestingly, other COXIBs, such as NS-398 or DFU had no effect on cell viability, being DFU a more selective inhibitor [59] and indicating that the protective role of celecoxib in hepatic fibrosis is not associated with COX-2 inhibition. In line with this, OSU-03012, a non-cyclooxygenase-inhibiting celecoxib derivative, promotes apoptosis and inhibits activation of LX-2 cells [60]. The deleterious effects of COX-2 inhibition on fibrosis progression were also reported in kidney [61] and lung [62]. The antifibrotic role of PGE_2 on pulmonary fibrosis is achieved by inhibiting fibroblast proliferation, synthesis of collagen and modulation of TGF-β-induced transition of fibroblasts to myofibroblasts [63]. To note, PGE_2 in lungs is normally present at much higher concentrations than in plasma, resembling the levels of constitutive COX-2 expression reached in hCOX-2-Tg animals. In line with this, it has been reported that PGE_2 down-regulated the expression of fibrosis-inducing genes in human fat explants from obese individuals as well as the fibrogenic response of differentiated adipocytes to the fibrogenic actions of TGF-β [64]. In the presence of COX-2, the protective effect is afforded in at least two ways: through the production of hepatoprotective prostaglandins [3] promoting tissue regeneration [65] and by downregulation of pro-

inflammatory cytokines which help tissue recovery by promoting resolution of inflammation [66].

These results shed new insights into a possible physiological protective mechanism of COX-2 induction in the progression of the NAFLD pathogenesis. This hypothesis is sustained in the fact that using hCOX-2-Tg mice we confirmed that continuously derived hepatic PGE_2 production plays a protective role against the development of NASH and hepatic fibrosis. Thus, our data suggest that the use of stable PG analogs or mimicking COX-2 signaling in the liver could represent a good therapeutic option to ameliorate NAFLD progression.

4.1. Conclusions

In our transgenic mouse model, we corroborated that constitutive hepatocyte COX-2 expression ameliorates NASH and liver fibrosis development by reducing inflammation, oxidative stress and apoptosis and by modulating activation of hepatic stellate cells, respectively. This data suggest a possible protective role for COX-2 induction in NASH/NAFLD progression.

Supplementary data to this article can be found online at http://dx.doi.org/10.1016/j.bbadis.2016.06.009.

Conflict of interest

The authors do not have any disclosures to report.

Funding

This work was supported by Financing Program for short stays abroad for Assistant Researchers (CONICET-Argentina) (2618/13) and ANPCyT-PICT 2383-2012 to D.F.; SAF2012-39732 (MINECO, Spain) and CIBERehd (ISCIII, Spain) (CB06/04/1069) to M.C.; SAF2014-52492 (MINECO, Spain) to L.B.; S2010/BMD-2378 (Comunidad de Madrid, CAM) to L.B. and P.M.S.; RD12/0042/0019 (ISCIII, Spain) and CIBERehd (ISCIII, Spain) to L.B. and P.M.S.; SAF-2015-65267-R (MINECO/FEDER), S2010/BMD-2423 (Comunidad de Madrid, CAM), EFSD and Amylin Paul Langerhans Grant and CIBERdem (ISCIII, Spain) to A.M.V.; PI13/01299 (ISCIII, Spain) to C.G-M.; SAF2013-43713-R (MINECO, Spain) to P.M.S.

Transparency document

The Transparency document associated with this article can be found, in the online version.

References

[1] E. Ricciotti, G.A. FitzGerald, Prostaglandins and inflammation, Arterioscler. Thromb. Vasc. Biol. 31 (2011) 986–1000, http://dx.doi.org/10.1161/ATVBAHA.110.207449.
[2] P. Martín-Sanz, N.A. Callejas, M. Casado, M.J. Díaz-Guerra, L. Boscá, Expression of cyclooxygenase-2 in foetal rat hepatocytes stimulated with lipopolysaccharide and pro-inflammatory cytokines, Br. J. Pharmacol. 125 (1998) 1313–1319, http://dx.doi.org/10.1038/sj.bjp.0702196.
[3] M. Casado, N.A. Callejas, J. Rodrigo, X. Zhao, S.K. Dey, L. Boscá, et al., Contribution of cyclooxygenase 2 to liver regeneration after partial hepatectomy, FASEB J. 15 (2001) 2016–2018, http://dx.doi.org/10.1096/fj.01-0158fje.
[4] A. Fernández-Alvarez, C. Llorente-Izquierdo, R. Mayoral, N. Agra, L. Boscá, M. Casado, et al., Evaluation of epigenetic modulation of cyclooxygenase-2 as a prognostic marker for hepatocellular carcinoma, Oncogenesis 1 (2012), e23 http://dx.doi.org/10.1038/oncsis.2012.23.
[5] R. Mayoral, B. Mollá, J.M. Flores, L. Boscá, M. Casado, P. Martín-Sanz, Constitutive expression of cyclooxygenase 2 transgene in hepatocytes protects against liver injury, Biochem. J. 416 (2008) 337–346, http://dx.doi.org/10.1042/BJ20081224.
[6] C.P. Day, Non-alcoholic fatty liver disease: a massive problem, Clin. Med. 11 (2011) 176–178.
[7] M. Masarone, A. Federico, L. Abenavoli, C. Loguercio, M. Persico, Non alcoholic fatty liver: epidemiology and natural history, Rev. Recent Clin. Trials 9 (2014) 126–133.
[8] F. Marra, A. Gastaldelli, G. Svegliati Baroni, G. Tell, C. Tiribelli, Molecular basis and mechanisms of progression of non-alcoholic steatohepatitis, Trends Mol. Med. 14 (2008) 72–81, http://dx.doi.org/10.1016/j.molmed.2007.12.003.
[9] C. García-Monzón, O. Lo Iacono, R. Mayoral, A. González-Rodríguez, M.E. Miquilena-Colina, T. Lozano-Rodríguez, et al., Hepatic insulin resistance is associated with increased apoptosis and fibrogenesis in nonalcoholic steatohepatitis and chronic hepatitis C, J. Hepatol. 54 (2011) 142–152, http://dx.doi.org/10.1016/j.jhep.2010.06.021.
[10] M. Asrih, F.R. Jornayvaz, Inflammation as a potential link between nonalcoholic fatty liver disease and insulin resistance, J. Endocrinol. 218 (2013) R25–R36, http://dx.doi.org/10.1530/JOE-13-0201.
[11] S.L. Friedman, Hepatic stellate cells: protean, multifunctional, and enigmatic cells of the liver, Physiol. Rev. 88 (2008) 125–172, http://dx.doi.org/10.1152/physrev.00013.2007.
[12] S.L. Friedman, Mechanisms of hepatic fibrogenesis, Gastroenterology 134 (2008) 1655–1669, http://dx.doi.org/10.1053/j.gastro.2008.03.003.
[13] A. Castilla, J. Prieto, N. Fausto, Transforming growth factors beta 1 and alpha in chronic liver disease. Effects of interferon alfa therapy, N. Engl. J. Med. 324 (1991) 933–940, http://dx.doi.org/10.1056/NEJM199104043241401.
[14] A.Y. Hui, A.J. Dannenberg, J.J.Y. Sung, K. Subbaramaiah, B. Du, P. Olinga, et al., Prostaglandin E2 inhibits transforming growth factor beta 1-mediated induction of collagen alpha 1(I) in hepatic stellate cells, J. Hepatol. 41 (2004) 251–258, http://dx.doi.org/10.1016/j.jhep.2004.04.033.
[15] S.M. Kim, K.C. Park, H.G. Kim, S.J. Han, Effect of selective cyclooxygenase-2 inhibitor meloxicam on liver fibrosis in rats with ligated common bile ducts, Hepatol. Res. 38 (2008) 800–809, http://dx.doi.org/10.1111/j.1872-034X.2008.00339.x.
[16] Y.-H. Paik, J.K. Kim, J.I. Lee, S.H. Kang, D.Y. Kim, S.H. An, et al., Celecoxib induces hepatic stellate cell apoptosis through inhibition of Akt activation and suppresses hepatic fibrosis in rats, Gut 58 (2009) 1517–1527, http://dx.doi.org/10.1136/gut.2008.157420.
[17] J. Yu, E. Ip, A. Dela Peña, J.Y. Hou, J. Sesha, N. Pera, et al., COX-2 induction in mice with experimental nutritional steatohepatitis: role as pro-inflammatory mediator, Hepatology 43 (2006) 826–836, http://dx.doi.org/10.1002/hep.21108.
[18] A.Y. Hui, W.K. Leung, H.L.Y. Chan, F.K.L. Chan, M.Y.Y. Go, K.K. Chan, et al., Effect of celecoxib on experimental liver fibrosis in rat, Liver Int. 26 (2006) 125–136, http://dx.doi.org/10.1111/j.1478-3231.2005.01202.x.
[19] Y. Kamada, K. Mori, H. Matsumoto, S. Kiso, Y. Yoshida, S. Shinzaki, et al., *N*-Acetylglucosaminyltransferase V regulates TGF-β response in hepatic stellate cells and the progression of steatohepatitis, Glycobiology 22 (2012) 778–787, http://dx.doi.org/10.1093/glycob/cws012.
[20] D.E. Francés, O. Motiño, N. Agrá, A. González-Rodríguez, A. Fernández-Álvarez, C. Cucarella, et al., Hepatic cyclooxygenase-2 expression protects against diet-induced steatosis, obesity and insulin resistance, Diabetes 64 (2015) 1522–1531, http://dx.doi.org/10.2337/db14-0979.
[21] M. Casado, B. Mollá, R. Roy, A. Fernández-Martínez, C. Cucarella, R. Mayoral, et al., Protection against Fas-induced liver apoptosis in transgenic mice expressing cyclooxygenase 2 in hepatocytes, Hepatology 45 (2007) 631–638, http://dx.doi.org/10.1002/hep.21556.
[22] V.G. Trusca, E.V. Fuior, I.C. Florea, D. Kardassis, M. Simionescu, A.V. Gafencu, Macrophage-specific up-regulation of apolipoprotein E gene expression by STAT1 is achieved via long range genomic interactions, J. Biol. Chem. 286 (2011) 13891–13904, http://dx.doi.org/10.1074/jbc.M110.179572.
[23] W. Liang, A.L. Menke, A. Driessen, G.H. Koek, J.H. Lindeman, R. Stoop, et al., Establishment of a general NAFLD scoring system for rodent models and comparison to human liver pathology, PLoS One 9 (2014), e115922 http://dx.doi.org/10.1371/journal.pone.0115922.
[24] V. Pardo, Á. González-Rodríguez, C. Guijas, J. Balsinde, Á.M. Valverde, Opposite cross-talk by oleate and palmitate on insulin signaling in hepatocytes through macrophage activation, J. Biol. Chem. 290 (2015) 11663–11677, http://dx.doi.org/10.1074/jbc.M115.649483.
[25] I. Mederacke, D.H. Dapito, S. Affò, H. Uchinami, R.F. Schwabe, High-yield and high-purity isolation of hepatic stellate cells from normal and fibrotic mouse livers, Nat. Protoc. 10 (2015) 305–315, http://dx.doi.org/10.1038/nprot.2015.017.
[26] C. Sanz-Garcia, G. Ferrer-Mayorga, A. Gonzalez-Rodriguez, A.M. Valverde, A. Martin-Duce, J.P. Velasco-Martin, et al., Sterile inflammation in acetaminophen-induced liver injury is mediated by Cot/tpl2, J. Biol. Chem. 288 (2013) 15342–15351, http://dx.doi.org/10.1074/jbc.M112.439547.
[27] M.M. Bradford, A rapid and sensitive method for the quantitation of microgram quantities of protein utilizing the principle of protein-dye binding, Anal. Biochem. 72 (1976) 248–254.
[28] D. Francés, M.T. Ronco, E. Ochoa, M.L. Alvarez, A. Quiroga, J.P. Parody, et al., Oxidative stress in primary culture hepatocytes isolated from partially hepatectomized rats, Can. J. Physiol. Pharmacol. 85 (2007) 1047–1051, http://dx.doi.org/10.1139/y07-087.
[29] H. Ohkawa, N. Ohishi, K. Yagi, Assay for lipid peroxides in animal tissues by thiobarbituric acid reaction, Anal. Biochem. 95 (1979) 351–358.
[30] D.E. Francés, M.T. Ronco, P.I. Ingaramo, J.A. Monti, G.B. Pisani, J.P. Parody, et al., Role of reactive oxygen species in the early stages of liver regeneration in streptozotocin-induced diabetic rats, Free Radic. Res. 45 (2011) 1143–1153, http://dx.doi.org/10.3109/10715762.2011.602345.
[31] F. Tietze, Enzymic method for quantitative determination of nanogram amounts of total and oxidized glutathione: applications to mammalian blood and other tissues, Anal. Biochem. 27 (1969) 502–522.
[32] C. Vandeputte, I. Guizon, I. Genestie-Denis, B. Vannier, G. Lorenzon, A microtiter plate assay for total glutathione and glutathione disulfide contents in cultured/isolated cells: performance study of a new miniaturized protocol, Cell Biol. Toxicol. 10 (1994) 415–421.
[33] S.H. Ibrahim, P. Hirsova, H. Malhi, G.J. Gores, Animal models of nonalcoholic steatohepatitis: eat, delete, and inflame, Dig. Dis. Sci. (2015) http://dx.doi.org/10.1007/s10620-015-3977-1.
[34] E. Mas, M. Danjoux, V. Garcia, S. Carpentier, B. Ségui, T. Levade, IL-6 deficiency attenuates murine diet-induced non-alcoholic steatohepatitis, PLoS One 4 (2009), e7929 http://dx.doi.org/10.1371/journal.pone.0007929.

[35] M.E. Rinella, M.S. Elias, R.R. Smolak, T. Fu, J. Borensztajn, R.M. Green, Mechanisms of hepatic steatosis in mice fed a lipogenic methionine choline-deficient diet, J. Lipid Res. 49 (2008) 1068–1076, http://dx.doi.org/10.1194/jlr.M800042-JLR200.
[36] C. Baeck, A. Wehr, K.R. Karlmark, F. Heymann, M. Vucur, N. Gassler, et al., Pharmacological inhibition of the chemokine CCL2 (MCP-1) diminishes liver macrophage infiltration and steatohepatitis in chronic hepatic injury, Gut 61 (2012) 416–426, http://dx.doi.org/10.1136/gutjnl-2011-300304.
[37] K.R. Karlmark, R. Weiskirchen, H.W. Zimmermann, N. Gassler, F. Ginhoux, C. Weber, et al., Hepatic recruitment of the inflammatory Gr1+ monocyte subset upon liver injury promotes hepatic fibrosis, Hepatology 50 (2009) 261–274, http://dx.doi.org/10.1002/hep.22950.
[38] K. Miura, L. Yang, N. van Rooijen, H. Ohnishi, E. Seki, Hepatic recruitment of macrophages promotes nonalcoholic steatohepatitis through CCR2, Am. J. Physiol. Gastrointest. Liver Physiol. 302 (2012) G1310–G1321, http://dx.doi.org/10.1152/ajpgi.00365.2011.
[39] H. Morinaga, R. Mayoral, J. Heinrichsdorff, O. Osborn, N. Franck, N. Hah, et al., Characterization of distinct subpopulations of hepatic macrophages in HFD/obese mice, Diabetes 64 (2015) 1120–1130, http://dx.doi.org/10.2337/db14-1238.
[40] D.E.a. Francés, P.I. Ingaramo, R. Mayoral, P. Través, M. Casado, Á.M. Valverde, et al., Cyclooxygenase-2 over-expression inhibits liver apoptosis induced by hyperglycemia, J. Cell. Biochem. 114 (2013) 669–680, http://dx.doi.org/10.1002/jcb.24409.
[41] I.A. Leclercq, G.C. Farrell, C. Sempoux, A. dela Peña, Y. Horsmans, Curcumin inhibits NF-kappaB activation and reduces the severity of experimental steatohepatitis in mice, J. Hepatol. 41 (2004) 926–934, http://dx.doi.org/10.1016/j.jhep.2004.08.010.
[42] L. Yang, Y.S. Roh, J. Song, B. Zhang, C. Liu, R. Loomba, et al., Transforming growth factor beta signaling in hepatocytes participates in steatohepatitis through regulation of cell death and lipid metabolism in mice, Hepatology 59 (2014) 483–495, http://dx.doi.org/10.1002/hep.26698.
[43] J.C. Bonner, Regulation of PDGF and its receptors in fibrotic diseases, Cytokine Growth Factor Rev. 15 (2004) 255–273, http://dx.doi.org/10.1016/j.cytogfr.2004.03.006.
[44] Q. Xu, M. Nakayama, Y. Suzuki, K. Sakai, T. Nakamura, Y. Sakai, et al., Suppression of acute hepatic injury by a synthetic prostacyclin agonist through hepatocyte growth factor expression, Am. J. Physiol. Gastrointest. Liver Physiol. 302 (2012) G420–G429, http://dx.doi.org/10.1152/ajpgi.00216.2011.
[45] J. Yu, C.W. Wu, E.S.H. Chu, A.Y. Hui, A.S.L. Cheng, M.Y.Y. Go, et al., Elucidation of the role of COX-2 in liver fibrogenesis using transgenic mice, Biochem. Biophys. Res. Commun. 372 (2008) 571–577, http://dx.doi.org/10.1016/j.bbrc.2008.05.069.
[46] O. Motiño, D.E. Francés, R. Mayoral, L. Castro-Sánchez, M. Fernández-Velasco, L. Boscá, et al., Regulation of MicroRNA 183 by cyclooxygenase 2 in liver is DEAD-box helicase p68 (DDX5) dependent: role in insulin signaling, Mol. Cell. Biol. 35 (2015) 2554–2567, http://dx.doi.org/10.1128/MCB.00198-15.
[47] Y. Takahashi, Y. Soejima, T. Fukusato, Animal models of nonalcoholic fatty liver disease/nonalcoholic steatohepatitis, World J. Gastroenterol. 18 (2012) 2300–2308, http://dx.doi.org/10.3748/wjg.v18.i19.2300.
[48] M.W. Rolfe, S.L. Kunkel, T.J. Standiford, M.B. Orringer, S.H. Phan, H.L. Evanoff, et al., Expression and regulation of human pulmonary fibroblast-derived monocyte chemotactic peptide-1, Am. J. Phys. 263 (1992) L536–L545.
[49] C. Mitchell, D. Couton, J.-P. Couty, M. Anson, A.-M. Crain, V. Bizet, et al., Dual role of CCR2 in the constitution and the resolution of liver fibrosis in mice, Am. J. Pathol. 174 (2009) 1766–1775, http://dx.doi.org/10.2353/ajpath.2009.080632.
[50] A.E. Obstfeld, E. Sugaru, M. Thearle, A.-M. Francisco, C. Gayet, H.N. Ginsberg, et al., C-C chemokine receptor 2 (CCR2) regulates the hepatic recruitment of myeloid cells that promote obesity-induced hepatic steatosis, Diabetes 59 (2010) 916–925, http://dx.doi.org/10.2337/db09-1403.
[51] S. Thapaliya, A. Wree, D. Povero, M.E. Inzaugarat, M. Berk, L. Dixon, et al., Caspase 3 inactivation protects against hepatic cell death and ameliorates fibrogenesis in a diet-induced NASH model, Dig. Dis. Sci. 59 (2014) 1197–1206, http://dx.doi.org/10.1007/s10620-014-3167-6.
[52] A. Fernández-Martínez, B. Mollá, R. Mayoral, L. Boscá, M. Casado, P. Martín-Sanz, Cyclooxygenase 2 expression impairs serum-withdrawal-induced apoptosis in liver cells, Biochem. J. 398 (2006) 371–380, http://dx.doi.org/10.1042/BJ20060780.
[53] B. Kroll, S. Kunz, N. Tu, L.R. Schwarz, Inhibition of transforming growth factor-beta1 and UV light-induced apoptosis by prostanoids in primary cultures of rat hepatocytes, Toxicol. Appl. Pharmacol. 152 (1998) 240–250, http://dx.doi.org/10.1006/taap.1998.8513.
[54] D.W. Beno, R. Espinal, B.M. Edelstein, B.H. Davis, Administration of prostaglandin E1 analog reduces rat hepatic and Ito cell collagen gene expression and collagen accumulation after bile duct ligation injury, Hepatology 17 (1993) 707–714.
[55] S.H. Wettlaufer, J.P. Scott, R.C. McEachin, M. Peters-Golden, S.K. Huang, Myofibroblast dedifferentiation by PGE2 is characterized by reversal of the global transcriptome, Am. J. Respir. Cell Mol. Biol. (2015) http://dx.doi.org/10.1165/rcmb.2014-0468OC.
[56] L.R.K. Penke, S.K. Huang, E.S. White, M. Peters-Golden, Prostaglandin E2 inhibits α-smooth muscle actin transcription during myofibroblast differentiation via distinct mechanisms of modulation of serum response factor and myocardin-related transcription factor-a, J. Biol. Chem. 289 (2014) 17151–17162, http://dx.doi.org/10.1074/jbc.M114.558130.
[57] E. Pomianowska, D. Sandnes, K. Grzyb, A.R. Schjølberg, M. Aasrum, I.H. Tveteraas, et al., Inhibitory effects of prostaglandin E2 on collagen synthesis and cell proliferation in human stellate cells from pancreatic head adenocarcinoma, BMC Cancer 14 (2014) 413, http://dx.doi.org/10.1186/1471-2407-14-413.
[58] S. Grosch, I. Tegeder, E. Niederberger, L. Brautigam, G. Geisslinger, COX-2 independent induction of cell cycle arrest and apoptosis in colon cancer cells by the selective COX-2 inhibitor celecoxib, FASEB J. 15 (2001) 2742–2744, http://dx.doi.org/10.1096/fj.01-0299fje.
[59] D. Riendeau, M.D. Percival, S. Boyce, C. Brideau, S. Charleson, W. Cromlish, et al., Biochemical and pharmacological profile of a tetrasubstituted furanone as a highly selective COX-2 inhibitor, Br. J. Pharmacol. 121 (1997) 105–117, http://dx.doi.org/10.1038/sj.bjp.0701076.
[60] J. Zhang, M. Wang, Z. Zhang, Z. Luo, F. Liu, J. Liu, Celecoxib derivative OSU-03012 inhibits the proliferation and activation of hepatic stellate cells by inducing cell senescence, Mol. Med. Rep. 11 (2015) 3021–3026, http://dx.doi.org/10.3892/mmr.2014.3048.
[61] M. Kamata, K. Hosono, T. Fujita, K. Kamata, M. Majima, Role of cyclooxygenase-2 in the development of interstitial fibrosis in kidneys following unilateral ureteral obstruction in mice, Biomed. Pharmacother. 70 (2015) 174–180, http://dx.doi.org/10.1016/j.biopha.2015.01.010.
[62] J.C. Bonner, A.B. Rice, J.L. Ingram, C.R. Moomaw, A. Nyska, A. Bradbury, et al., Susceptibility of cyclooxygenase-2-deficient mice to pulmonary fibrogenesis, Am. J. Pathol. 161 (2002) 459–470, http://dx.doi.org/10.1016/S0002-9440(10)64202-2.
[63] C. Vancheri, C. Mastruzzo, M.A. Sortino, N. Crimi, The lung as a privileged site for the beneficial actions of PGE2, Trends Immunol. 25 (2004) 40–46.
[64] V. García-Alonso, E. Titos, J. Alcaraz-Quiles, B. Rius, A. Lopategi, C. López-Vicario, et al., Prostaglandin E2 exerts multiple regulatory actions on human obese adipose tissue remodeling, inflammation, adaptive thermogenesis and lipolysis, PLoS One 11 (2016), e0153751 http://dx.doi.org/10.1371/journal.pone.0153751.
[65] Y. Zhang, A. Desai, S.Y. Yang, K.B. Bae, M.I. Antczak, S.P. Fink, et al., Inhibition of the prostaglandin-degrading enzyme 15-PGDH potentiates tissue regeneration, Science 348 (6240) (2015) http://dx.doi.org/10.1126/science.aaa2340 aaa2340-1-2340-8.
[66] P.R. Colville-Nash, D.W. Gilroy, Cyclooxygenase enzymes as targets for therapeutic intervention in inflammation, Drug News Perspect. 13 (2000) 587–597.